

M. Hino<sup>1</sup>, T.Oda<sup>1</sup>, H.Endo<sup>2</sup>, K.Mori<sup>1</sup>, F. Funama<sup>3</sup>, Y. Kawabata<sup>1</sup>

<sup>1</sup>*Institute for Integrated Radiation and Nuclear Science, Kyoto University (KURNS), Japan*

<sup>2</sup>*IMSS, KEK, Japan*

<sup>3</sup>*Dept., Nucl. Eng., Kyoto University, Japan*

**INTRODUCTION:** Magnetic multilayer mirror consisting of ferromagnetic layers and nonmagnetic layers is useful to polarize neutron beam. As a polarizing neutron device, larger saturation magnetization of the ferromagnetic layers with lower applied magnetic field is very important. In this sense, pure iron (Fe) is good material. Fe-Co alloy, known as Permendur, is very good material and it had used for many neutron research establishments. Recently brightness of neutron beam has been really increased, and magnetic multilayer contained cobalt is not suitable due to the activation of the element for modern intense neutron facility. The radioactivation of Fe due to neutron irradiation is less serious than the other ferromagnetic materials. Silicon (Si), germanium (Ge) and these compounds are generally used for the nonmagnetic layers because the neutron scattering length density (SLD) of Fe for down spin neutrons. We also have already succeeded in fabricating  $m \sim 5$  Fe/SiGe polarizing neutron supermirrors with high reflectivity using an ion beam sputtering instrument (KUR-IBS) installed to the Institute for Integrated Radiation and Nuclear Science, Kyoto University (KURNS) [1,2]. These polarizing supermirrors have been used as polarizer and analyzer at neutron resonance spin echo spectrometer at BL06 in Materials and Life Science Experimental Facility (MLF), Japan Proton Accelerator Research Complex (J-PARC). The SiGe layer is obtained by simultaneous deposition of Si and Ge target. The composition ratio of Si and Ge is possible to be controlled by changing geometrical configuration of Si and Ge target. Recently detailed investigation of Fe/Si and Fe/Ge multilayer fabricated by ion beam sputtering was reported [3]. The fine-tuning of scattering length density of nonmagnetic material is still very important for high performance polarizing supermirror. With use of the KUR-IBS, SiGe layer tends to be slightly rough comparing with Si and SiC layers by using X-ray reflectometer. Carbon (C) is very good element because they have low incoherent and absorption cross section with less radioactivation. The composition ratio of Si and C is also possible to be controlled by changing geometrical configuration of silicon and carbon target.

#### EXPERIMENTS:

Figure 1 shows measured hysteresis loops for the Fe/SiC(Si) polarizing supermirror with typical two sample geometry, A and B. After the measurement of A, the sample was rotated by 90 degrees and the measurement of B was conducted. The sample size is about 8 mm in square and the magnetization measurement was conducted with vibrating sample magnetometer of the KURNS. It indicates that there is no in-plane anisotropy and applied magnetic field of 30 mT is possible to satu-

rate magnetically the polarizing supermirror.

**RESULTS:** Figure 2 shows up and down spin neutron reflectivities by the Fe/SiC(Si) polarizing supermirror under an external field of 60 mT. The reflectivity with high- $m$  area ( $m > 3$ ) was relatively high although the flipping ratio was not so high. The reflectivity of up spin neutrons was rapidly reduced around low- $m$  area ( $1 < m < 3$ ). This result supported that the SLD of SiC layer was not so equaled to that of Fe for down spin neutrons. In fact, the SLD of SiC layer was much larger than that of SiGe layer and that layer depended on geometrical configuration of silicon and carbon target. In other words, it indicates that the Fe/SiC(Si) polarizing supermirror is still of great potential for improvement. The accurate SLD of SiC layer with various sputtering condition and the improved performance of larger- $m$  Fe/SiC(Si) polarizing supermirror will be reported in our future.

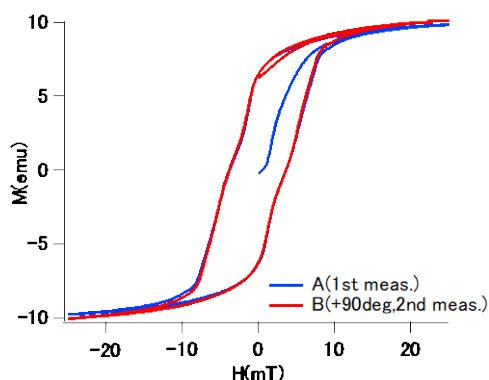


Fig. 1. Measured hysteresis loops of the Fe/SiC(Si) supermirror with two set angle.

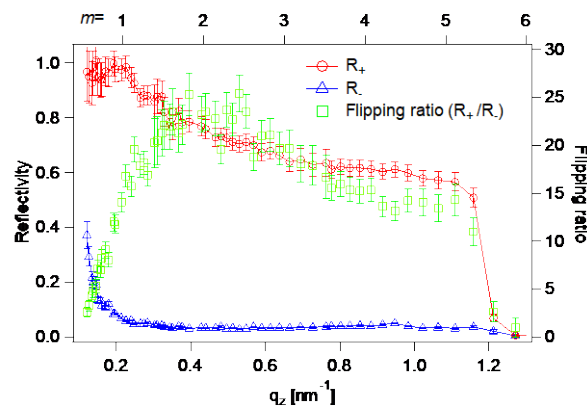


Fig. 2. Polarized neutron reflectivity profiles of the Fe/SiC(Si) polarizing supermirror for spin-up (○) and down (△) neutrons. Here  $m = q_z / Q_c$ , where  $Q_c = 0.217 \text{ nm}^{-1}$ .

#### REFERENCES:

- [1] M.Hino, *et al.*, Physica B 385&386, 1187(2006).
- [2] M.Hino, *et al.*, Nucl. Instr. and Meth., **797**(2015) 265.
- [3] R.Maruyama, *et al.*, Nucl. Instr. and Meth., **888**, (2018) 70.

## CO1-2 Current Status of Versatile Compact Neutron Diffractometer (VCND) on the B-3 Beam Port of KUR, 2020

K. Mori, R. Okumura, H. Yoshino, H. Nakamura, S. Sato<sup>1</sup>, K. Iwase<sup>2</sup>, Y. Oba<sup>3</sup>, Y. Kaneko<sup>3</sup>

*Institute for Integrated Radiation and Nuclear Science, Kyoto University (KURNS)*

<sup>1</sup>*High Energy Accelerator Research Organization (KEK)*

<sup>2</sup>*Department of Materials and Engineering, Ibaraki University*

<sup>3</sup>*Materials Sciences Research Center, Japan Atomic Energy Agency (JAEA)*

**INTRODUCTION:** Neutron diffraction is a powerful tool to precisely determine the positions of light elements (e.g., hydrogen and lithium) in solids. This is the main reason why neutron powder diffractometers are critical for structural investigations of energy storage materials, for example, rechargeable lithium-ion batteries and hydrogen-absorbing materials. The B-3 beam port of Kyoto University Research Reactor (KUR) had long been used as a four-circle single-crystal neutron diffractometer (4CND). For the last decade, however, the 4CND was so old that its research activity on neutron science was quite low. Now, the versatile compact neutron diffractometer (VCND) is installed on the B-3 beam port of KUR [1].

**SPECIFICATIONS:** Fig. 1 shows the current state of the VCND. The neutron wavelength,  $\lambda$ , which is monochromatized by the (220) plane of a Cu single crystal (i.e., Cu monochromator), is 1.0 Å. To cover the detector area of  $6^\circ \leq 2\theta \leq 130^\circ$ , twenty-five <sup>3</sup>He tube detectors (1/2 inch in diameter) are used, where  $2\theta$  is the scattering angle. A detector bank including twenty-five <sup>3</sup>He tube detectors is placed on the arm of the HUBER-440 goniometer. The distance from the Cu monochromator to the sample is approximately 2 m, and the distance from the sample to the detector is 1.2 m.

**CRYSTAL STRUCTURE ANALYSIS:** The lanthanum-nickel intermetallic alloy (LaNi<sub>5</sub>) is well known as a conventional hydrogen-absorbing material. Fig. 2 shows the Rietveld refinement using neutron diffraction data for LaNi<sub>5</sub> at room temperature, where  $\Delta 2\theta = 0.1^\circ$ . In this figure, an excellent fit was obtained between the observed and calculated intensities; the atomic positions, La (0, 0, 0) in the 1a site, Ni1 (1/3, 2/3, 0) in the 2c site, and Ni2 (1/2, 0, 1/2) in the 3g site, were used to refine its crystal structure based on the space group *P6/mmm* (hexagonal system). Consequently, the lattice parameters, *a* and *c*, were estimated to be 5.04(7) and 4.01(4) Å, respectively.

### REFERENCE

1. K. Mori, R. Okumura, H. Yoshino, M. Kanayama, S. Satoh, Y. Oba, K. Iwase, H. Hiraka, M. Hino, T. Sano, Y. Kawabata, T. Kamiyama, T. Otomo, T. Fukunaga, Commissioning of versatile compact neutron diffractometer (VCND) at the B-3 beam port of Kyoto University Research Reactor (KUR), *JPS Conference Proceedings*, 33 (2021) 011093.

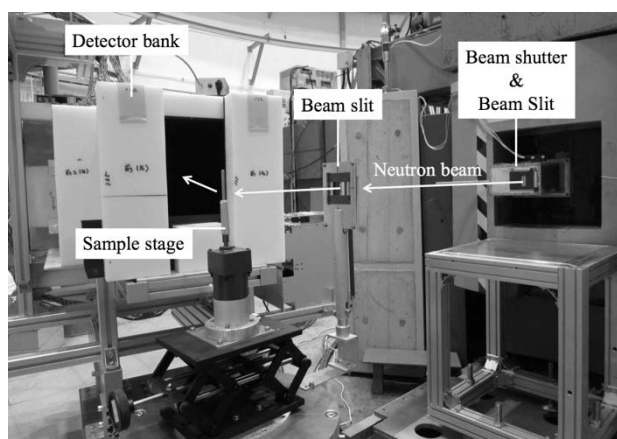


Fig. 1. Versatile compact neutron diffractometer (VCND) installed at the B-3 beam port of Kyoto University Research Reactor (KUR) [1].

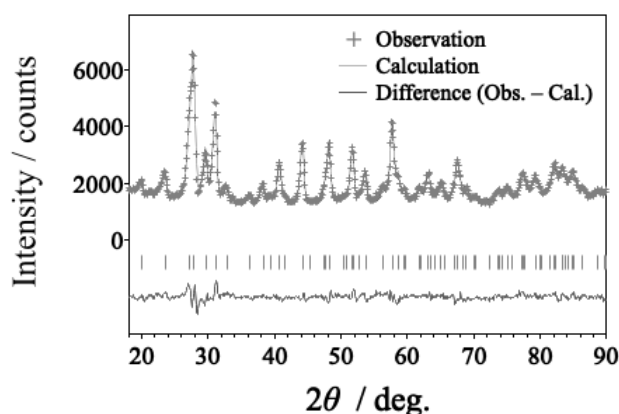


Fig. 2. The crystal structure refinement of LaNi<sub>5</sub> using neutron diffraction data collected at the VCND.

## CO1-3 Radius of Gyration of Polymer for Viscosity Index Improver at Various Temperatures Evaluated by Small-Angle X-Ray and Neutron Scatterings

T. Hirayama, R. Takahashi<sup>1</sup>, Y. Takashima<sup>2</sup>, K. Tamura<sup>2</sup>, N. Sato<sup>3</sup>, M. Sugiyama<sup>3</sup>, S. Takada<sup>4</sup>

*Dept. of Mechanical Eng. and Science, Graduate School of Kyoto University*

<sup>1</sup>*Dept. of Mechanical Eng., Graduate School of Doshisha University*

<sup>2</sup>*Idemitsu Kosan Co., Ltd.*

<sup>3</sup>*Institute for Integrated Radiation and Nuclear Science, Kyoto University*

<sup>4</sup>*Japan Atomic Energy Agency*

**INTRODUCTION:** Lubricating oils are necessary for friction reduction and high wear durability of sliding surfaces in machine components, and the development of the best oils is strongly required from industry. Viscosity index improver (VII) is a kind of additives for relieving the reduction of viscosity of lubricating oil due to temperature rise. Classical textbooks say that the VII molecules work with changing their equivalent radius in base oil in accordance with oil temperature. However, there are only few papers investigating the equivalent radius of VII molecules by small-angle X-ray scattering (SAXS) and/or small-angle neutron scattering (SANS)<sup>[1]</sup>, and there is still room for discussion of the behavior and working mechanism of VII molecules in oil. This study tried to investigate the radius of gyration of comb-shaped VII polymers in base oil at various temperatures by SAXS and SANS, and the behavior of polymers was discussed.

**EXPERIMENT:** To investigate the radius of gyration of VII polymer, we used a SAXS instrument (NANOPIX, Rigaku) with a Cu-target X-ray source emitting X-ray with a wavelength of 1.54 Å, a characteristic line of Cu-Kα. The 1.2 mm-thick aluminum cell having optical windows made of 20-μm thermally-resistant engineering plastic film (Superio-UT, Mitsubishi chemical) was used for the measurement. The cell temperature increased to be 25, 40, 60, 80 and 100°C in turn, and the last measurement was carried out at 25°C again after cooling for checking if the VII molecule degenerated or not by heat. Poly(methyl acrylate) (PMA) type VII in comb-shape, as shown in Fig. 1, was prepared as a typical one used in engine oil in the study. Squalane was used as a model base oil, and the concentrations of PMA into squalane were 0.5, 1.0 and 2.0 mass%.

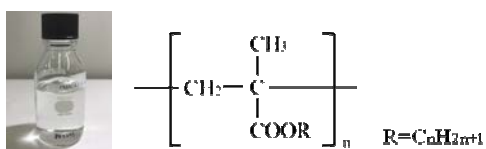


Fig. 1. Chemical structure of Comb-shaped PMA.

**RESULTS AND DISCUSSION:** The SAXS intensity profiles versus scattering vector  $q$  from squalane with 0.5 and 2.0 mass%-PMA type VII at each temperature were shown in Fig. 2, for example. The profiles were obtained by subtracting the intensity profiles from pure squalane at each temperature previously measured with the same liquid cell. We can see that the intensity profiles changed in accordance with the temperature rise. The trend of profile change was similar with the profile obtained by SANS, as shown in the right in Fig. 2. The radius of gyration of this polymer was not possible to be estimated from the profiles because of the profile change. From the whole measurement, we found on the behaviour of comb-shaped PMA in squalane that the shrunk polymers aggregate as ‘multimer’ in oil at low temperature, but they swell and separate to be ‘unimer’ in the random coil state at high temperature, resulting in contributing to the viscosity increase of oil, as shown in Fig. 3. Both of X-ray and neutron small-angle scatterings were effective for structural analysis of polymer in oil. Particularly, Kratky plot by SANS was the most powerful for the estimation of molecular structure of VII even in oil.

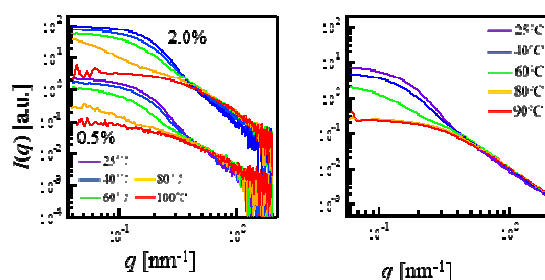


Fig. 2. SAXS profiles from squalane with 0.5 and 2.0 mass% Comb-shaped PMA at various temperatures. (Left: SAXS, right: SANS)

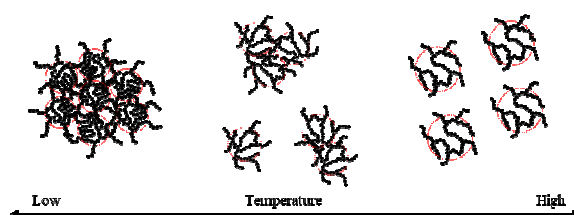


Fig. 3. Structure of comb-shaped PMA with temperature change.

### REFERENCES:

- [1] M. J. Covitch, K. J. Trickett, How Polymers Behave as Viscosity Index Improvers in Lubricating Oils, *Adv. Chem. Eng. Sci.*, 5 (2015) 134.

## CO1-4 Development of High-resolution cold/ultracold neutron detectors using nuclear emulsion

N. Naganawa, M. Hino<sup>1</sup>, K. Hirota<sup>2</sup>, H. Kawahara<sup>2</sup>, M. Kimura<sup>3,4</sup>, M. Kitaguchi<sup>2,5</sup>, K. Mishima<sup>6,7</sup>, A. Muncem<sup>8</sup>, N. Muto<sup>2</sup>, M. Nakagawa<sup>8</sup>, T. R. Saito<sup>8</sup>, A. Umemoto<sup>2</sup>, and J. Yoshida<sup>8</sup>

*Institute of Materials and Systems for Sustainability,  
Nagoya University,*

<sup>1</sup>*Institute for Integrated Radiation and Nuclear Science,  
Kyoto University*

<sup>2</sup>*Graduate School of Science, Nagoya University*

<sup>3</sup>*Nagoya Proton Therapy Center, Nagoya City University  
West Medical Center*

<sup>4</sup>*Graduate School of Medical Sciences, Nagoya City  
University*

<sup>5</sup>*Kobayashi-Maskawa Institute for Origin of Particles  
and the Universe (KMI), Nagoya University,*

<sup>6</sup>*High Energy Accelerator Research Organization (KEK)*

<sup>7</sup>*J-PARC Center*

<sup>8</sup>*High Energy Nuclear Physics Laboratory, Cluster for  
Pioneering Research, RIKEN*

**INTRODUCTION:** Nuclear emulsion can be used as slow neutron detectors by combining it with thin layers including nuclide which convert neutrons to ionizing particles or adding such nuclide into emulsion layers. We conducted two experiments, Experiment 1 and 2, using the former and the latter type of detector, respectively. The former type whose spatial resolution was estimated to be finer than 100 nm was developed [1]. It can be a novel device for neutron imaging. In this detector, neutrons are detected by the emission of  $\alpha$  particles or  ${}^7\text{Li}$  nuclei from the neutron capture reaction,  ${}^{10}\text{B}+n\rightarrow\alpha+{}^7\text{Li}$ , by  ${}^{10}\text{B}$  in the converter layer. One can observe their tracks as series of silver grains under an epi-illumination optical microscope. The lengths of these tracks are approximately 5 and 2  $\mu\text{m}$ , respectively. In the Experiment 1, detectors were produced by sputtering  ${}^{10}\text{B}_4\text{C}$  (200 nm)-NiC-C layers on Si substrate using ion beam sputtering system [2] at KURRI and applying the fine-grained nuclear emulsion [3] at Nagoya University. We produced several samples that recorded tracks at different densities of them to develop track recognition method that can be applied to various densities of tracks. The latter type of detector can be used for fundamental studies of radiation therapies. We are applying it to the study of the mechanism of proton boron capture therapy (PBCT). The therapy was proposed to improve the dose concentration of proton cancer therapy using  ${}^{11}\text{B}(p,\alpha)2\alpha$  reaction. For the study, a fine-grained nuclear emulsion added of natural boron will be developed for the detection of  $\alpha$  particles emitted from the reaction point. A uniformity of the distribution of the boron has to be checked. In order to check it, Experiment 2 was conducted. Sodium pentaborate was added to fine-grained nuclear emulsion to introduce boron in it. The emulsion was exposed to neutrons and tracks of  $\alpha$  particles and  ${}^7\text{Li}$  from reaction  ${}^{10}\text{B}+n\rightarrow\alpha+{}^7\text{Li}$  were counted.

**EXPERIMENT 1:** Neutron irradiations were conducted at the CN3 beamline at KURRI. The detectors were individually packed in a light-tight film and placed

directly downstream of the neutron guide tube. Irradiations of 1000 s, 10000 s, and 25000 s were conducted under 1 MW thermal power of the reactor. The detectors were developed and observed under the microscope.

**RESULTS:**  $390\pm 16$  tracks per 100  $\mu\text{m}^2$  were observed in the sample for irradiation of 1000 s as shown in Fig.1. Assuming a neutron flux of  $7.6\times 10^5$  / $\text{cm}^2/\text{sec}$  at the window of the neutron guide tube [4], the neutron conversion efficiency was calculated to be approximately 0.5%. We have scanned these detectors with an optical microscope to obtain a dataset of sample images. Using these images, we are developing image processing for track recognition.



Fig. 1. One of the microscopic images of the detector that recorded tracks of  $\alpha$  particle and  ${}^7\text{Li}$  from neutron absorption by  ${}^{10}\text{B}$ . The dimension of field of view was  $50\times 50\ \mu\text{m}^2$ . About 120 tracks were recorded in this area by 1000 seconds of neutron irradiation.

**EXPERIMENT 2:** The sample consists of fine-grained emulsion with  $\text{Na}_2\text{B}_{10}\text{O}_{16}\cdot 10\text{H}_2\text{O}$  added by a concentration of  $1\times 10^{-1}$  mol/L. The film was then exposed to 20 meV neutrons at the CN3 beamline. The beam density was  $5\times 10^8$  / $\text{cm}^2$ . The exposed film was developed and observed under an epi-illumination optical microscope.

**RESULTS:** The frequency of the  ${}^{10}\text{B}+n\rightarrow\alpha+{}^7\text{Li}$  reaction in the exposed emulsion was expected to be 4 per  $100\times 100\ \mu\text{m}^2$  from the amount of sodium pentaborate and the reaction cross-section. The number of the candidate events was  $3.1\pm 0.6$  per  $100\times 100\ \mu\text{m}^2$ , which was approximately consistent with the expected one. The reactions were distributed uniformly within statistical error along the depth in the emulsion layer. The results indicated that sodium pentaborate is uniformly distributed.

### REFERENCES:

- [1] N. Naganawa *et al.*, *Eur. Phys. J. C.* **78** (2018) 959.
- [2] M. Hino *et al.*, *Nucl. Instrum. Methods Phys. Res. A* **797**, 265–270 (2015).
- [3] T. Asada *et al.*, *Prog. Theor. Exp. Phys.* **2017**, 2017, 063H01.
- [4] M. Hino *et al.*, *Annu. Rep. Res. React. Inst. Kyoto Univ.* **27** (1994) 196-204.

## CO1-5 Optimization of neutron spin flipper with large beam acceptance

M. Kitaguchi, K. Morikawa<sup>1</sup>, T. Hasegawa<sup>1</sup>, T. Oda<sup>2</sup>, and M. Hino<sup>2</sup>

KMI, Nagoya University

<sup>1</sup>Graduate School of Science, Nagoya University

<sup>2</sup>Institute for Integrated Radiation and Nuclear Science, Kyoto University

**INTRODUCTION:** The recent values of neutron lifetime deviate far beyond the systematic errors claimed in the past and require the further improvement for the neutron lifetime puzzle. We are continuing neutron lifetime measurement at the polarized beam branch of the NOP beamline installed at the port BL05 in J-PARC. The system consists of a neutron chopper (SFC) and a gas chamber (TPC) for detecting the electrons from the neutron beta decays. The TPC contains small amount of  $^3\text{He}$ . The rate of the  $^3\text{He}(n,p)^3\text{H}$  reaction is measured by counting the protons. The neutron lifetime is measured as the ratio of the electron events to the proton events [1].

The large background via neutron-induced reactions is suppressed by introducing small neutron bunches into the TPC and selectively detecting decay electrons and reaction protons only when neutron bunches are traveling inside the sensitive volume and they were not transmitting through chamber windows and other materials on the beam path. The SFC is a spin-selective optics to switch the neutron beam using the combination of magnetic supermirrors and spin flippers[2]. Polarized neutrons are injected into the SFC. Controlling the timing of spin-flip makes neutron bunches at the exit of the SFC, which can be reflected by the magnetic mirrors successively. By employing the triple series reflection, the present version of the SFC chops the neutron beam with the intensity contrast of about 400. During the lifetime measurement, the bunch length is adjusted as about 50 cm, which is half of the length of TPC sensitive region for maximizing the signal statistics. The cross section of the output bunches is 2 cm  $\times$  2 cm. In order to reduce the statistical uncertainties for the lifetime measurement to the order of 1 s, the incident neutron flux into the TPC must be increased. Although the new mirrors have been already assembled to accept large cross section of the neutron beam, large scale of spin flippers are also required. New mirrors and flippers with the beam acceptance of 3 cm  $\times$  3 cm can transfer neutrons with the intensity of 4 times larger than that before upgrade.

**EXPERIMENTS AND RESULTS:** We have tried to install the SFC with large mirrors and flippers into the NOP beamline (fig.1). The magnetic mirrors are kept in the strong magnetic field in order to be saturated. The field is leaking to the flipper position and has the influence on the flipping probability of neutron spin. We measured the distribution of the magnetic field around

the flippers. We demonstrated that the probability can be improved by the proper correction of the field with the additional coils. We are now doing optimization of the shape of the flipper coils based on the simulations and experiments performed at CN3 in KUR.

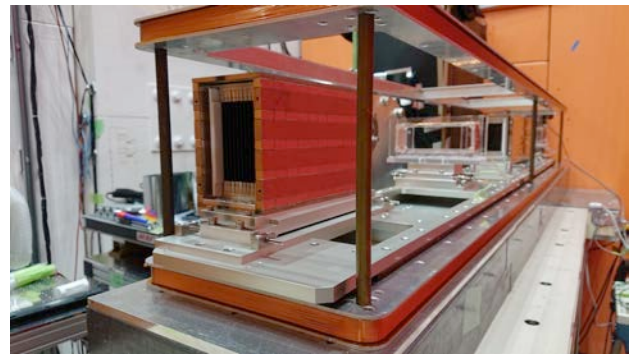


Figure 1: Spin Flip Chopper with large beam acceptance installed into NOP beamline in J-PARC.

### REFERENCES:

- [1] K Hirota, et al., Prog. Theor. Exp. Phys., 2020, 123C02 (2020).
- [2] K. Taketani et al., Nucl. Instr. and Meth. A634 (2011) S134–S137.

## CO1-6 Development of multilayer mirrors for neutron interferometer

M. Kitaguchi, T. Fujiie<sup>1</sup>, T. Oda<sup>2</sup>, and M. Hino<sup>2</sup>

KMI, Nagoya University

<sup>1</sup>Graduate School of Science, Nagoya University

<sup>2</sup>Institute for Integrated Radiation and Nuclear Science, Kyoto University

**INTRODUCTION:** Neutron interferometry is a powerful technique for studying fundamental physics. Numerous interesting experiments [1] have been performed since the first successful test of a single-crystal neutron interferometer [2]. However, the single-crystal interferometer is inherently not able to deal with a neutron that has a wavelength longer than twice its lattice constant. In order to investigate problems of fundamental physics, including tests of quantum measurement theories and searches for non-Newtonian effects of gravitation, the interferometry of cold neutrons is extremely important, since the sensitivity of interferometer for small interaction increases with the neutron wavelength. A large scale of interferometer also has the advantage to increase the sensitivity to small interactions.

One of the solutions is an interferometer using neutron multilayer mirrors [3]. We succeeded in developing a multilayer interferometer for cold neutrons in which two paths are completely separated for the first time using wide-gap etalons [4]. We can easily control parameters such as Bragg angle, reflectivity, and Bragg peak width by selecting the deposited material and tuning the bilayer thickness and the number of layers.

We have started the development of multilayer interferometer at the beamline 05 NOP in MLF. In 2019, we demonstrated the interference fringes with etalons with monochromatic mirrors. Figure 1 shows the interference fringes with etalons according to time-of-flight. The phase of interferogram depends on the wavelength of neutrons. Because the mirrors have narrow bandwidth of the neutron reflectivity, the number of neutrons contributing to the interference is limited. When the neutron supermirrors whose lattice constants vary gradually are utilized in the interferometer, the effective range of neutron wavelength can be broadened to be applicable to a pulsed source. In addition, the wavelength dependence of the interactions can be measured simultaneously by using pulsed neutrons.

**EXPERIMENTS AND RESULTS:** We are trying to fabricate the neutron mirrors with wide band for the interferometer by using Ion Beam Sputtering facility in KURNS. The mirrors should have the wide and smooth top of the reflectivity with the range of momentum transfer from  $0.4 \text{ nm}^{-1}$  to  $1.0 \text{ nm}^{-1}$ . Especially, half mirrors with the wide range of neutron wavelength are needed for the interferometer. We tried to make the half mirrors and to measure the reflectivity at CN3 in KUR.

Figure 2 shows the reflectivity of the half mirror with 538 layers on the fused silica substrate. We are continuing the development of the mirrors for the neutron interferometer.

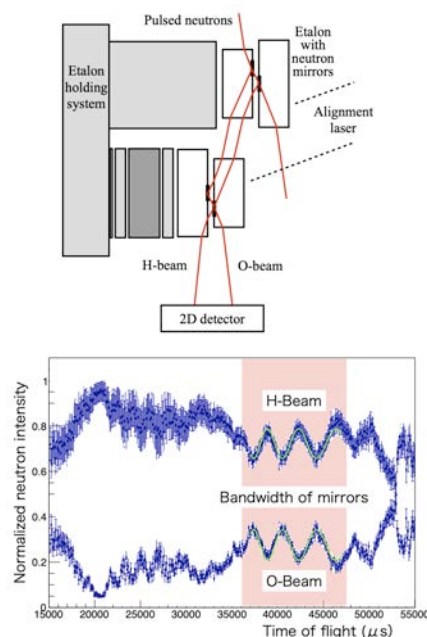


Figure 1: Interference fringes with multilayer mirrors for pulsed neutrons.

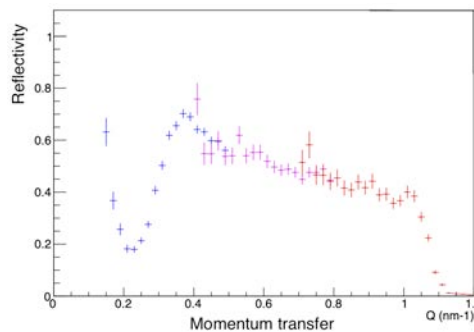


Figure 2: Reflectivity of the half mirror with wide band of neutron wavelength.

### REFERENCES:

- [1] H. Rauch and S. Werner, Neutron Interferometry Oxford University Press, Oxford, 2000;
- [2] J. Byrne, Neutron, Nuclei and Matter Institute of Physics Publishing, London, 1994, Chap. 7;
- [3] Mater Wave Interferometry, edited by G. Badurek, H. Rauch, and A. Zeilinger North-Holland, Amsterdam, 1988.
- [4] H. Rauch, W. Treimer, and U. Bonse, Phys. Lett. 47A, 369 (1974).
- [5] M. Kitaguchi, et al., Phys. Rev. A 67, 033609 (2003).
- [6] Y. Seki, et al., J. Phys. Soc. Jpn. 79, 124201 (2010).